Inorganic Chemistry

Article

pubs.acs.org/IC

Aqueous Complexes for Efficient Size-based Separation of Americium from Curium

Mark P. Jensen,*[,†] Renato Chiarizia,[†] Ilya A. Shkrob,[†] Joseph S. Ulicki,[‡] Brian D. Spindler,[‡] Daniel J. Murphy,[‡] Mahmun Hossain,[‡] Adrián Roca-Sabio,[§] Carlos Platas-Iglesias,[§] Andrés de Blas,[§] and Teresa Rodríguez-Blas*[,§]

[†]Chemical Sciences and Engineering Division, Argonne National Laboratory, 9700 S. Cass Ave., Argonne, Illinois 60439, United States

[‡]Department of Chemistry and Biochemistry, University of Wisconsin—Milwaukee, Milwaukee, Wisconsin 53201, United States

[§]Departamento de Química Fundamental, Universidade da Coruña, Campus da Zapateira, Rúa da Fraga no. 10, 15008 A Coruña, Spain

Supporting Information

ABSTRACT: Complexation of the adjacent actinide ions americium(III) and curium(III) by the ligand *N*,*N*′-bis[(6-carboxy-2-pyridyl)methyl]-1,10-diaza-18-crown-6 (H_2bp18c6) in aqueous solution was studied to quantify and characterize its americium/curium selectivity. Liquid−liquid extraction and spectrophotometric titration indicated the presence of both fully deprotonated and monoprotonated complexes, An(bp18c6)$^+$ and An(Hbp18c6)$^{2+}$ (An = Am or Cm), at the acidities that would be encountered when treating nuclear wastes. The stability constants of the complexes in 1 M $NaNO_3$ determined using competitive complexation were log β_{101} = 15.49 ± 0.06 for Am and 14.88 ± 0.03 for Cm, indicating a reversal of the usual order of complex stability, where ligands bind the smaller Cm^{III} ion more tightly than Am^{III}. The Am/Cm selectivity of bp18c6^{2-} that is defined by the ratio of the Am and Cm stability constants (β_{101} Am/β_{101} Cm = 4.1) is the largest reported so far for binary An^{III}−ligand complexes. Theoretical density functional theory calculations using the B3LYP functional suggest that the ligand's size-selectivity for larger 4f- and 5f-element cations arises from steric constraints in the crown ether ring. Enhanced 5f character in molecular orbitals involving actinide−nitrogen interactions is predicted to favor actinide(III) complexation by bp18c6^{2-} over the complexation of similarly sized lanthanide(III) cations.

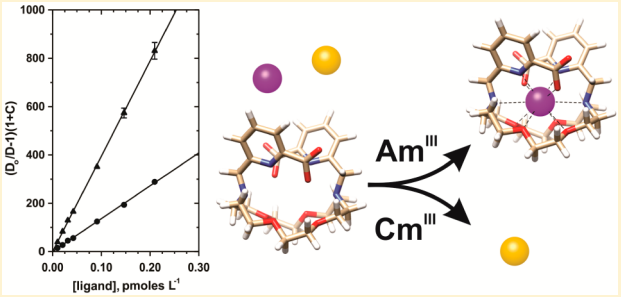

INTRODUCTION

Separation of the adjacent actinide (An) elements americium and curium is important in concepts for advanced nuclear fuel cycles proposed to reduce the transuranic content of nuclear waste placed in geological repositories,[1] but the similar chemistries of Am and Cm make this separation among the most difficult in the periodic table.[2] Am and Cm are normally present as trivalent ions in aqueous solution. Consequently, the separation of americium from curium after selective oxidation to form Am^{IV}, Am^{V}, or Am^{VI}[3,4] and the separation of Am^{III} from Cm^{III} using chromatography[5] have been proposed. However, the higher oxidation states of Am are all strong oxidants with standard reduction potentials that exceed +1.7 V in acidic aqueous solutions,[3] which makes it difficult to generate and maintain these species in realistic separation systems.[6] It is also technically challenging to couple chromatographic separations with the continuous liquid−liquid extraction processes favored for large-scale nuclear separations. A ligand system that selectively binds either Am^{III} or Cm^{III} could offer substantial advantages over chromatographic or redox-based process-scale separations.[7]

Trivalent Am and Cm are difficult to separate because they possess the same charge, are nearly the same size,[8] and both the metal-centered orbitals and the 5f valence electrons generally contribute little to the bonding properties of transplutonium actinide ions, making their metal−ligand bonds primarily electrostatic (ionic) in nature.[9] Consequently, as for the trivalent lanthanide (Ln) ions, much of the periodic variation in the thermodynamic strength of An^{III}−ligand complexes arises from variations in the size of the actinide ions.[10]

The small difference in the ionic radii of Am^{III} and Cm^{III} represents the principal means for chemically distinguishing between these cations. Analogous to the well-known lanthanide contraction, relativistic effects and incomplete shielding of the actinide 5f electrons causes the radii of An^{III} ions to contract progressively as the atomic number increases,[11] and the

Received: January 30, 2014
Published: June 3, 2014

   dx.doi.org/10.1021/ic500244p | *Inorg. Chem.* 2014, 53, 6003−6012

trivalent ions of both the lanthanide and the actinide series span similar ranges of ionic radii. Therefore, Cm^{III} is slightly smaller than Am^{III} (1.094 Å for Cm^{3+} vs. 1.106 Å for Am^{3+} with CN 8),[8] and the Cm^{III} cation possesses a correspondingly larger charge density than Am^{III}. Because of this, the Gibbs free energies of complexation for Cm–ligand complexes are typically reported to be 0.5–2 kJ·mol^{-1} more favorable than those of the corresponding Am–ligand complexes[12] when steric constraints are not important. This behavior is similar to that observed for complexes of adjacent Ln^{III} ions.

While such slight free energy differences between complexes can be used in a size-based chemical sorting of Cm^{III} from Am^{III} by repeating a separation many times, *efficient* Am/Cm separations require free energy differences on the order of 6–12 kJ·mol^{-1} or more. We have examined strategies for enhancing size-based Am/Cm selectivity by incorporating inter- or intraligand steric constraints in ternary complexes in order to favor complexation of the *larger* cation (Am^{III}), reversing the expected order of complex stability[13] and producing Am^{III} complexes that are more stable than the corresponding Cm^{III} complexes.[14] However, the ternary complexes studied exhibited only a partial reversal in selectivity. In contrast, recent work in lanthanide complexation[15,16] suggests that sterically constrained macrocyclic ligands that form binary complexes with trivalent f-element cations can provide an efficient system for maximizing the complexation free energy differences between Am^{III} and Cm^{III}. To understand the potential of such ligands for Am/Cm separation, we studied the Am^{III} and Cm^{III} complexes formed by the dianion of the ligand *N*,*N*′-bis[(6-carboxy-2-pyridyl)methyl]-1,10-diaza-18-crown-6 (H_2bp18c6, Figure 1), which is known to be selective

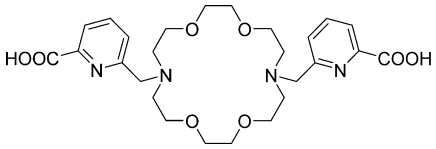

Figure 1. Structural formula of H_2bp18c6.

for larger Ln^{III} cations.[15] In addition to its documented size-selectivity, the bp18c6^{2-} dianion also possesses four potential nitrogen donor sites, which could impart important selectivity for An^{III} over Ln^{III}.[17]

In this study, we demonstrate that bp18c6^{2-} exhibits substantial selectivity for Am^{III} over Cm^{III} and the lanthanide cation Eu^{III}. Further characterization of the complexes using density functional theory (DFT) calculations carried out using the B3LYP functional implies that bp18c6^{2-} possesses both size-based selectivity for trivalent actinide cations and enhanced electronic interactions between nitrogen donor atoms in the ligand and the actinide cations that favor complexation of An^{III} cations over similarly sized Ln^{III} cations.

EXPERIMENTAL SECTION

Materials. The synthesis of H_2bp18c6 has been described previously.[15] The ligand produced by this procedure was further purified by washing an aqueous solution of the hydrochloride salt of H_2bp18c6 with heptane followed by precipitation with acetone. The purity of the resulting material (≥98%) was verified using ^{1}H and ^{13}C NMR, mass spectrometry, potentiometric pH titration, and Karl Fischer titration. Weighed amounts of the purified ligand were then dissolved in aqueous solutions.

All commercial reagents except the extractants bis(2-ethylhexyl)-phosphoric acid (Hdehp) and tri-*n*-butylphosphate (TBP) were used as received. The purification of Hdehp[18] and TBP[19] followed literature procedures. The ionic strength of the aqueous solutions was maintained at 1.0 M with $NaNO_3$ (≥99.0%). Nitric acid (Ultrex grade) and 50% (w/w) NaOH were diluted, standardized by titration to the phenolphthalein end point, and used for titrations, to adjust the acidity of the ligand solutions and to calibrate the pH electrode.

Caution! *The isotopes ^{152,154}Eu, ^{241}Am, ^{243}Am, and ^{244}Cm are radioactive and must be handled in facilities designed to safely handle these materials.*

The radionuclides ^{152,154}Eu, ^{241}Am, ^{243}Am, and ^{244}Cm were taken from Argonne National Laboratory stocks. The stock solutions of ^{152,154}Eu and ^{241}Am required no additional purification. They were evaporated to dryness and dissolved in 0.01 M HNO_3 to yield solutions containing 4 × 10^4 dpm Am/μL and 2 × 10^5 dpm Eu/μL. The ^{243}Am stock (99.87 atom % ^{243}Am, 0.13 atom % ^{241}Am, and 0.005 atom % ^{244}Cm by α-spectroscopy) was purified as previously described[20] and dissolved in 0.01 M HCl. The short half-life of ^{244}Cm ($t_{1/2}$ = 18.11 years) necessitated removal of the ^{240}Pu decay product for accurate distribution ratio measurements. The Cm solution was adjusted to 5 M HNO_3 and contacted four times with an equal volume of fresh, pre-equilibrated 30% tri-*n*-butylphosphate in heptane. The resulting aqueous phase was washed twice with two volumes of heptane, evaporated to dryness, and dissolved in 0.01 M HNO_3 to give a solution containing 8 × 10^4 dpm Cm/μL. The resulting Cm had a radiochemical purity ≥99.96%, as determined by α-spectroscopy.

Titration. All titrations were carried out in glass reaction vessels thermostated at 25.0 ± 0.1 °C. Potentiometric titrations were conducted under a N_2 atmosphere with a computer controlled Radiometer ABU91 buret equipped with an antidiffusion buret tip. A ROSS combination glass pH electrode (Thermo Scientific) filled with 3 M NaCl was calibrated to read pcH (pcH = −log H^+ concentration in mol/L) by daily potentiometric titration of 0.01 M HNO_3/0.99 M $NaNO_3$ between pcH 2 and 12 with 40 additions of 0.1 M NaOH/0.9 M $NaNO_3$. Small day to day variations in the junction potential were observed, but the electrode slope remained constant at 98.85 ± 0.13% of the Nernstian value throughout the course of the titrations. (Throughout this work, all uncertainties are reported at the 95% confidence level.) The pK_a values of the ligand in 1 M $NaNO_3$ were determined from triplicate titrations of 4 × 10^{-3} M solutions of H_2bp18c6 containing a known amount of excess HNO_3 by standardized 0.1 M NaOH/0.9 M $NaNO_3$. The run-to-run reproducibility was ±0.006 pcH units.

A spectrophotometric pcH titration of a mixture of 2.3 × 10^{-4} M ^{243}Am and 2.4 × 10^{-4} M H_2bp18c6 in 0.1 M HNO_3/0.9 M $NaNO_3$ was conducted as previously described,[21] monitoring the Am absorption between 495 and 530 nm using a 1.000 cm path length cell. The titration vessel was maintained at 25.0 ± 0.2 °C, while the spectrometer compartment was thermostated at 25.0 ± 0.5 °C. The americium concentration was determined at the end of the titration by liquid scintillation counting with α/β discrimination.

Liquid–Liquid Extraction. The stability constants of the Am^{III}–bp18c6^{2-} and Cm^{III}–bp18c6^{2-} complexes were measured by competitive complexation through liquid–liquid extraction. Equal volumes of pre-equilibrated organic phase containing a constant concentration of Hdehp in *o*-xylene and aqueous phases containing a variable amount of H_2bp18c6 (0–1 × 10^{-3} M) in 1 M $NaNO_3$ at a known pcH and ^{241}Am (2 × 10^{-7} M) or ^{244}Cm (8 × 10^{-9} M) were mixed for 1 h at 25 ± 1 °C. This time was determined to be sufficient to reach equilibrium in separate extraction kinetics experiments (Figure S1, Supporting Information). The two phases for each extraction condition were separated, and an aliquot was taken from each phase to determine the distribution ratio D_M, which is the ratio of the total concentration of the metal cation, M, in the organic phase to the total concentration of this metal cation in the aqueous phase, $D_M = [M]_{org}/[M]_{aq}$. The ^{244}Cm content of each phase was determined by liquid scintillation counting (Supporting Information), while the ^{241}Am content was determined by counting its 59 keV γ-emission with

dx.doi.org/10.1021/ic500244p | Inorg. Chem. 2014, 53, 6003–6012

Table 1. Logarithmic Protonation Constants Determined Using Potentiometry and Metal Complex Stability Constants Determined Using Distribution Measurements in 1 M $NaNO_3$ at 25 °C

reaction	constant	H	Am	Cm	Eu	literature
$H^+ + bp18c6^{2-}$	$pK_{a,4}$	8.05 ± 0.01				7.41,[a] 7.52[b]
$H^+ + Hbp18c6^-$	$pK_{a,3}$	6.58 ± 0.01				6.85,[a] 7.03[b]
$H^+ + H_2bp18c6$	$pK_{a,2}$	3.45 ± 0.02				3.32,[a] 3.58[b]
$H^+ + H_3bp18c6^+$	$pK_{a,1}$	2.68 ± 0.02				2.36,[a] 2.47[b]
$M^{3+} + bp18c6^{2-}$	$\log \beta_{101}$		15.49 ± 0.06	14.88 ± 0.03	14.29 ± 0.15	13.01 (Eu)[a]
$M^{3+} + H^+ + bp18c6^{2-}$	$\log \beta_{111}$		17.68 ± 0.23	17.66 ± 0.08	16.26 ± 0.25	14.98 (Eu)[a]

[a]0.1 M KCl, 25 °C; ref 15, $pK_{a,5}$ = 1.69 also reported. [b]0.1 M KNO_3, 25 °C; ref 30.

a NaI detector. The desired pcH for a given set of ligand concentrations was maintained by the presence of 0.05 M sodium lactate/lactic acid buffer in the aqueous phases, and the equilibrium pcH was determined with a glass electrode. Parallel measurements of Eu^{III} distribution at pcH 2.88 using gamma counting of $^{152,154}Eu$ were also performed for comparison. The distributions ratios of the stable lanthanides La–Gd (except Pm) were also determined following the same equilibration procedures. The aqueous phases initially contained 1×10^{-5} M of each lanthanide, and the concentration of each lanthanide was determined by ICP-MS of both phases after the equilibrated organic phases were stripped with two volumes of 2 M HNO_3.

Computational Methods. All calculations were performed employing hybrid DFT with the B3LYP exchange-correlation functional,[22] and the Gaussian 09 package (revision A.02).[23] Full geometry optimizations of the $Ln(bp18c6)^+$ (Ln = Nd, Sm, Gd) and $An(bp18c6)^+$ (An = Am, Cm) complexes were performed by using the standard 6-31G(d) basis set for C, H, N, and O atoms. For the actinides (An = Am or Cm) (14s 13p 10d 8f)/[10s 9p 5d 4f] segmented valence basis sets with Stuttgart–Bonn variety relativistic effective core potentials (RECPs) were used,[24] while a (14s 13p 10d 8f)/[10s 8p 5d 4f] segmented valence basis set[25] with a Stuttgart–Bonn RECP[26] was used for each lanthanide (Ln = Nd, Sm, or Gd). The input geometries used were taken from the optimized geometries calculated for the lanthanide complexes previously reported.[15] No symmetry constraints were imposed during the optimizations. The default values for the integration grid ("fine") and the self-consistent field (SCF) energy convergence criteria (10^{-8}) were used. In these computations, the highest spin state was considered the ground state for all complexes. Since geometry optimizations were performed using a spin-unrestricted model, spin contamination[27] was assessed through a comparison of the expected difference between $S(S + 1)$ for the assigned spin state and the actual value of $\langle S^2 \rangle$.[28] The results (Table S1, Supporting Information) indicate that spin contamination is negligible for the Nd, Am, and Cm complexes and relatively small for the Sm and Gd analogues. Convergence of the SCF procedure during geometry optimizations of the Sm, Gd, and Am complexes was problematic, and therefore a quadratically convergent SCF procedure was used when first order SCF did not achieve convergence. The stationary points found on the potential energy surfaces as a result of the geometry optimizations have been established as energy minima rather than saddle points using vibrational frequency analysis. The relative Gibbs free energies of the different conformations of $Cm(bp18c6)^+$ were obtained at 25.00 °C (i.e., 298.15 K) within the harmonic approximation, and they include nonpotential-energy contributions (zero point energies and thermal terms) obtained through the same frequency analysis.

RESULTS

Binding Constants of $bp18c6^{2-}$. The protonation constants of $bp18c6^{2-}$ in 1 M $NaNO_3$ were determined by potentiometric titration. The results of three independent titrations between pcH 2.15 and 11.45 (n = 329 total data points) were combined and fit using the program PSEQUAD.[29] Four proton dissociation equilibria were detected by potentiometry under these conditions. The corresponding pK_a values obtained for the reactions

$$H_hbp18c6^{(h-2)} \rightleftharpoons H^+ + H_{h-1}bp18c6^{(h-3)} \quad (1)$$

($K_{a,(5-h)} = [H^+][H_{h-1}bp18c6^{(h-3)}][H_hbp18c6^{(h-2)}]^{-1}$, h = 1–4) are summarized in Table 1. These pK_a values in 1 M $NaNO_3$ are in good agreement with the pK_a values previously reported for this ligand[15,30] when the differences in ionic strength and nature of the background electrolyte are considered.

The stability constants for the Am^{III} and Cm^{III} complexes with $bp18c6^{2-}$ in 1 M $NaNO_3$ were determined using a biphasic competitive complexation technique[31] to quantify the ligand's selectivity for the Am^{III}/Cm^{III} pair. The distribution of Am or Cm was measured between an organic phase containing a fixed concentration of the lipophilic complexant Hdehp and aqueous phases containing varying total concentrations of $H_2bp18c6$ at four different equilibrium aqueous acidities (pcH = 2.58, 2.88, 3.10, and 3.31). Representative distribution ratios are depicted in Figure S1 in the Supporting Information.

Four classes of competing equilibria were considered in determining the stability constants from the experimental distribution data,

$$M^{3+} + H_hbp18c6^{(h-2)} \rightleftharpoons M(H_xbp18c6)^{(3+x-2)} + (h - x)H^+ \quad (2)$$

$$M^{3+} + 3(Hdehp)_{2,org} \rightleftharpoons M(H(dehp)_2)_{3,org} + 3H^+ \quad (3)$$

$$M^{3+} + NO_3^- \rightleftharpoons M(NO_3)^{2+} \quad (4)$$

and

$$M^{3+} + mlac^- \rightleftharpoons M(lac)_m^{(3-m)} \quad (m = 1, 2, \text{or } 3) \quad (5)$$

where the subscript org indicates species present in the organic phase, h is the average number of protons bound to uncomplexed $bp18c6^{2-}$, x is the average number of protons bound to complexed $bp18c6^{2-}$, and lac^- represents the lactate anion. The corresponding equilibrium constants for equilibria 2–5 are denoted as K_{bp18c6}, K_{ex}, $\beta_1^{NO_3^-}$, and β_m^{lac}, respectively. The ligand-to-metal stoichiometries of equilibria 2 and 3 were verified by slope analysis of the distribution data.[32] The measured $(Hdehp)_2$/metal stoichiometry was 2.9 ± 0.1, and the average measured bp18c6/metal stoichiometry was 1.0 ± 0.1, over the entire range of concentrations and acidities studied (Figure S1 and Table S2 in the Supporting Information).

The distribution ratio expression for this system of equilibria is

dx.doi.org/10.1021/ic500244p | Inorg. Chem. 2014, 53, 6003–6012

$$D_M = \left([M(H(dehp)_2)_3]_{org}\right)/\left([M^{3+}] + [M(NO_3)^{2+}] + [M(lac)_m^{(3-m)}]_{total} + [M(H_x bp18c6)^{(3+x-2)}]\right) \quad (6)$$

which can be recast as

$$D_M = \left(K_{ex}[(Hdehp)_2]_{org}[H^+]^{-3}\right) \Big/ \left(1 + \beta_1^{NO_3^-}[NO_3^-] + \sum_{m=1}^{3} \beta_m^{lac}[lac^-]^m + K_{bp18c6}[H_h bp18c6^{(h-2)}][H^+]^{(h-x)}\right) \quad (7)$$

by substituting the equilibrium constant expressions from equilibria 2−5. Because the total concentrations of Hdehp, NO_3^-, and lactate are constant and the pcH is fixed for a given set of titration measurements, one can further define the distribution ratio of a given metal ion in the absence of the ligand (i.e., $[H_h bp18c6^{(h-2)}] = 0$) at a particular pcH as D_0. The distribution ratio expression for a given set of measurements then simplifies to

$$\left(\frac{D_0}{D_M} - 1\right)(1 + C) = \beta^{app}[bp18c6^{2-}] \quad (8)$$

where $C = \beta_1^{NO_3^-}[NO_3^-] + \Sigma_{m=1}^{3}\beta_m^{lac}[lac^-]^m$ and $\beta^{app} = K_{bp18c6}[H^+]^x/\Pi_{i=4}^{(5-h)}K_{a,i}$ $(1 \le h \le 4)$. The values used for $\beta_1^{NO_3^-}$ and β_m^{lac} are given in Table S3, Supporting Information. Computation of the apparent stability constant of each metal−bp18c6^{2-} complex, β^{app}, from eq 8 by error-weighted least-squares regression is illustrated in Figure 2.

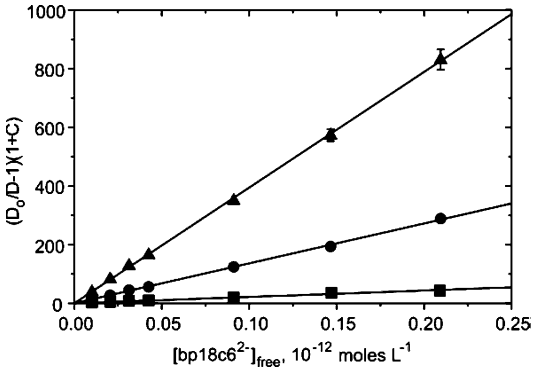

Figure 2. Determination of β^{app} for the (▲) Am, (●) Cm, and (■) Eu complexes of bp18c6^{2-} from distribution data at pcH 2.88. Error bars are shown when the uncertainty is larger than the symbol in the plot. The corresponding distribution ratios can be found in Figure S1c, Supporting Information.

While β^{app} is constant at a particular pcH, β^{app} is only independent of acidity if the complexes formed do not contain dissociable protons (i.e., $x = 0$ in equilibrium 2 and eq 8). Combining the data from the distribution measurements at different pcH values (Figure 3) demonstrates that β^{app}, the y intercept of the log−log plots of eq 8, varies with acidity. Additional slope analysis of the metal-to-proton stoichiometry[33] revealed the presence of both M(bp18c6)$^+$ and

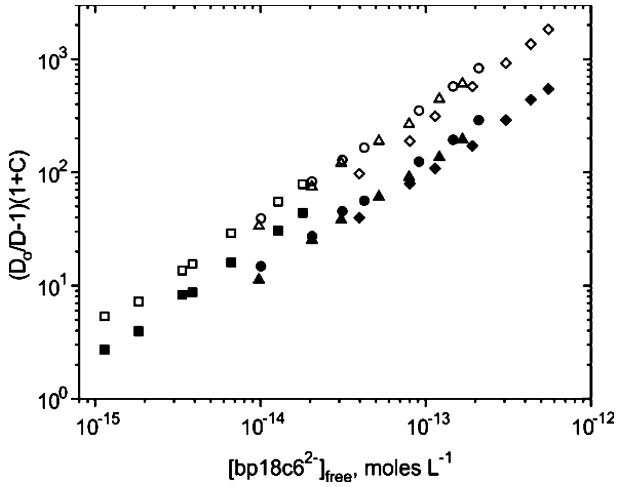

Figure 3. Variation in β^{app} of An^{III}−bp18c6^{2-} complexes with different pcH values: (■) 2.58, (●) 2.88, (▲) 3.10, and (♦) 3.31. Open symbols represent Am complexes, and closed symbols represent Cm complexes. The data would have formed two lines, one for each metal, had not protonated complexes formed in the aqueous solution (i.e., $\beta_{111} = 0$ and $\beta^{app} = \beta_{101}$).

M(Hbp18c6)$^{2+}$ complexes, as previously reported from potentiometric studies of lanthanide−bp18c6 complexes.[15] Thus, β^{app} can be expressed in terms of the stability constants of two equilibria[34]

$$M^{3+} + bp18c6^{2-} \rightleftharpoons M(bp18c6)^+ \quad (9)$$

$$M^{3+} + H^+ + bp18c6^{2-} \rightleftharpoons M(Hbp18c6)^{2+} \quad (10)$$

which are β_{101} and β_{111}, respectively. The resulting expression is

$$\beta^{app} = \beta_{101} + \beta_{111}[H^+] \quad (11)$$

The variation in the apparent stability constants with $[H^+]$ was used to determine values of β_{101} and β_{111} for Am and Cm, which are summarized in Table 1.

The americium complexes were further examined using spectrophotometric titration, monitoring the changes in the absorption spectra of the Am ion (Figure 4). Systematically

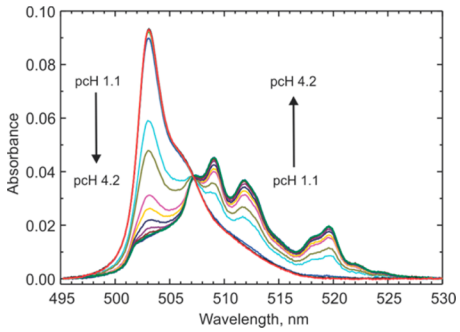

Figure 4. Spectrophotometric pcH titration of 0.23 mM Am-bp18c6^{2-} complexes in 1 M $NaNO_3$ at 25 °C.

increasing the concentration of bp18c6^{2-} available for metal complexation by increasing the pcH caused the absorption of Am^{3+} at 503 nm to decrease while new absorption bands with peaks at 509, 512, and 520 nm appeared. The apparent isosbestic point at 507.2 nm was not well-defined, implying the presence of more than two unique absorbing species. Both

dx.doi.org/10.1021/ic500244p | Inorg. Chem. 2014, 53, 6003−6012

principal component analysis[35] and matrix triangularization rank analysis[36] of the absorption spectra suggested the presence of three unique absorbing species.

The solution species were further studied by fitting the complete set of absorption spectra (14 spectra, 351 wavelengths per spectrum) to different speciation models based on equilibria 2 and 4. The program SQUAD[37] was used to determine the molar absorptivities and stability constants of the Am−bp18c6 complex(es) that best fit the experimental spectra for each model. As implied by the principal component analysis, the best fitting models always included *both* the $Am(bp18c6)^{+}$ and $Am(Hbp18c6)^{2+}$ complexes (Figure S2, Supporting Information). The reduced χ^2 of models including only $Am(bp18c6)^{+}$ or $Am(Hbp18c6)^{2+}$ were always greater than corresponding models containing both species, and the apparent β_{101} or β_{111} values calculated from the data using these single-complex models also were significantly greater than those derived from the distribution experiments. In contrast, the stability constants from the best-fitting two-complex model agreed with the distribution data, yielding values of log β_{101} = 15.65 ± 0.02 and log β_{111} = 17.83 ± 0.03. As expected, the spectra of the two Am−bp18c6 complexes (Figure S2a, Supporting Information) are similar since the stoichiometries of these two Am complexes differ only with respect to ligand protonation, which most likely involves a noncoordinated oxygen atom of a picolinate group. Indeed, it has been shown that protonation of the picolinate unit in other metal complexes does not provoke the partial decoordination of the ligand, and therefore ligand protonation does not cause important changes in the metal coordination environment.[38]

Structural and Electronic Analyses. Selected $Ln(bp18c6)^{+}$ and $An(bp18c6)^{+}$ complexes were modeled using DFT calculations in order to gain insight into the structural origins of the size-selectivity of $bp18c6^{2-}$ and potential differences in the electronic structures for the lanthanide(III) and actinide(III) complexes. In our previous study,[15] $Ln(bp18c6)^{+}$ complexes were modeled using the large core relativistic effective core potentials (RECP) of Dolg et al.,[39] and the related [5s4p3d]-GTO valence basis set was used to model the lanthanide complexes. That effective core potential includes 46 + $4f^n$ electrons in the core, leaving the outermost 11 electrons to be treated explicitly. In that study, the use of large core RECPs was justified by the expectation that the lanthanide 4f orbitals do not significantly contribute to bonding due to their limited radial extension as compared to the 5d and 6s shells. Other computational studies have compared the covalent contribution to bonding of analogous lanthanide and actinide complexes.[40] Those studies revealed that the 5f orbitals in actinide complexes can play a significant role in bonding, while the participation of 4f orbitals of lanthanides in bonding appears to be minimal or even negligible.[41] Herewith, for the sake of consistency we employed small-core RECPs to describe both the lanthanide and actinide complexes. The Nd^{III} and Sm^{III} complexes were examined because as they are the stable lanthanide ions closest in size to Am^{III} and Cm^{III},[8,42] while $Gd(bp18c6)^{+}$ was examined because Gd^{III} and Cm^{III} both have f^7 ground states.

When complexed to an An^{III} or Ln^{III} cation, the $bp18c6^{2-}$ ligand can potentially form eight diasteroisomeric forms that are consistent with the C_2 symmetry suggested by solution NMR spectroscopy.[15] These isomers result from combinations of the different helicities associated with the layout of the picolinate pendant arms (absolute configuration Δ or Λ) and the six five-membered chelate rings formed by the binding of the crown moiety (each of them showing absolute configuration δ or λ).[43] A conformational analysis performed on the $Cm(bp18c6)^{+}$ system shows that two conformations [$\Delta(\lambda\delta\lambda)$-$(\lambda\delta\lambda)$ and $\Delta(\delta\lambda\delta)(\delta\lambda\delta)$] are considerably more stable than the remaining ones (7.8−28.6 kJ·mol^{-1}), in agreement with our previous calculations on lanthanide complexes.[15] Thus, only these two geometries were considered in the case of the Nd, Sm, Gd, and Am complexes. Unfortunately, the geometry optimization of the $\Delta(\lambda\delta\lambda)(\lambda\delta\lambda)$ form of the Gd and Am complexes did not achieve convergence, and therefore the relative energy of the $\Delta(\delta\lambda\delta)(\delta\lambda\delta)$ and $\Delta(\lambda\delta\lambda)(\lambda\delta\lambda)$ isomers could not be determined for these cations. According to our calculations, the $\Delta(\delta\lambda\delta)(\delta\lambda\delta)$ conformation is slightly more stable than the $\Delta(\lambda\delta\lambda)(\lambda\delta\lambda)$ one for all complexes with convergent calculations [1.16 (Cm), 9.76 (Nd), and 0.15 (Sm) kJ·mol^{-1}]. The minimum energy conformation obtained for the $Cm(bp18c6)^{+}$ complex is shown in Figure 5. The optimized geometries show two different Ln−crown ether oxygen bond distances, as expected for C_2 symmetry (Table 2), and the computed structures agree with those of the minimum energy conformation predicted by previous calculations using a large-core RECP for the large Ln^{III} ions.[15]

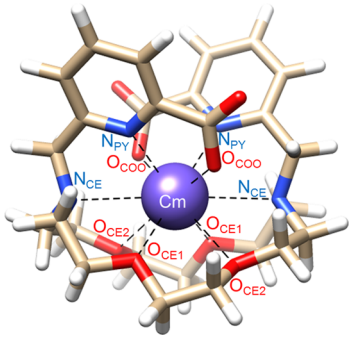

Figure 5. DFT optimized structure of $Cm(bp18c6)^{+}$ in the $\Delta(\delta\lambda\delta)(\delta\lambda\delta)$ conformation.

Table 2. Calculated Mean Bond Distances (Å) of the Metal Coordination Environments for the $\Delta(\delta\lambda\delta)(\delta\lambda\delta)$ Conformation $Ln(bp18c6)^{+}$ and $An(bp18c6)^{+}$ Complexes Using Small-Core RECP at the B3LYP/6-31G(d) Level[a]

	Nd	Sm	Gd	Am	Cm
M−N_{CE}	3.028	3.029	3.048	3.038	3.015
M−N_{PY}	2.647	2.630	2.613	2.639	2.628
M−O_{COO}	2.273	2.243	2.219	2.279	2.290
M−O_{CE1}	2.756	2.747	2.746	2.783	2.755
M−O_{CE2}	2.891	2.882	2.935	2.880	2.903

[a] N_{CE} = crown ether amine nitrogen atoms, N_{PY} = pyridyl nitrogen atoms, O_{COO} = carboxylate oxygen atoms, and O_{CE} = crown oxygen atoms as labeled in Figure 5.

The ionic radius of Am^{III} or Cm^{III} is very close to that of Nd^{III} or Sm^{III}, respectively (differing by <0.015 Å). As expected from this similarity, the bond distances calculated with the small-core RECP for the Am^{III}/Nd^{III} and Cm^{III}/Sm^{III} complexes are also quite similar. Interestingly, some of the M−O distances (M−O_{COO} and M−O_{CE2}, see Table 2) are longer for the Cm^{III} complex than for the Am^{III} complex, even though Cm^{III} is the smaller cation. This suggests a better match

dx.doi.org/10.1021/ic500244p | Inorg. Chem. 2014, 53, 6003−6012

between the donor atoms offered by the ligand and the larger Am^{III} ion. A lengthening of several Ln^{III}–donor distances with decreasing ionic radius of the Ln^{III} ion was previously shown to be consistent with the observed selectivity of $bp18c6^{2-}$ for the large lanthanides.

To gain further insight into the nature of chemical bonding in $bp18c6^{2-}$ complexes, population analyses were also performed. The computed Mulliken and atomic polar tensor (APT)[44] metallic charges, as well as the metallic spin densities (ρ_M) are given in Table 3. The Mulliken atomic charges are considerably smaller than the formal oxidation state of the metal ion, although Mulliken population analysis (MPA) usually overestimates this effect. However, the APT metallic charges are also considerably smaller than +3, implying a certain ligand-to-metal donation. The APT charges computed for each of the lanthanide and actinide complexes are very similar, indicating a similar degree of ligand-to-metal donation in all complexes investigated. The ρ_M values reflect the difference between the total α and β electronic calculations in spin-unrestricted calculations. As expected, the ρ_M values are close to those expected for the corresponding f^n states of the metallic center, implying the absence of metal-to-ligand back-donation in these complexes.

Table 3. Charges on Coordinated Metals from Mulliken and APT Analyses and the Metallic Spin Densities (ρ_M) for the $\Delta(\delta\lambda\delta)(\delta\lambda\delta)$ Conformation of the $Ln(bp18c6)^+$ and $An(bp18c6)^+$ Complexes

	Mulliken	APT	ρ_M
Nd ($4f^3$)	+1.39	+2.57	3.04
Sm ($4f^5$)	+1.38	+2.54	5.09
Gd ($4f^7$)	+1.32	+2.54	7.20
Am ($5f^6$)	+1.32	+2.53	6.07
Cm ($5f^7$)	+1.32	+2.59	6.99

A comparison of the electronic structure of isoelectronic and isostructural 4f and 5f complexes can assess the degree of covalence in the metal–ligand interactions. Thus, a molecular orbital (MO) analysis was carried out for isoelectronic (f^7) $Cm(bp18c6)^+$ and $Gd(bp18c6)^+$ complexes. Figure 6 shows density-of-states (DOS) and overlap population density-of-states (ODOS) plots obtained for the $Cm(bp18c6)^+$ and $Gd(bp18c6)^+$ systems from MPA.[45] The DOS diagrams shown in Figure 6 were generated from the contributions of the metal f orbitals, the non-f metal orbitals, and the ligand. Figure 6 also presents ODOS plots generated by considering two molecular fragments consisting of the metallic atom and the ligand and, therefore, provides information on the bonding character of MOs with respect to the metal–ligand interaction.

The MOs with important 5f contribution in the Cm^{III} complex have orbital energies between −12.2 and −11.3 eV, while the MOs with dominant 4f contribution in the Gd^{III} isoelectronic complex are between −13.4 and −13.0 eV, as may be expected from general considerations. The ODOS plot indicates that these gadolinium molecular orbitals are not significantly involved in covalent interactions with the ligand donor atoms. On the other hand, the ODOS plot for the α-spin orbitals in the Cm^{III} system indicates that the metal 5f orbitals are significantly involved in covalent bonding interaction with the ligand. Indeed, several MOs with Cm^{III} 5f contribution exhibit relatively large overlap populations with the ligand. As an example, Figure 7 shows a representation of α MO number

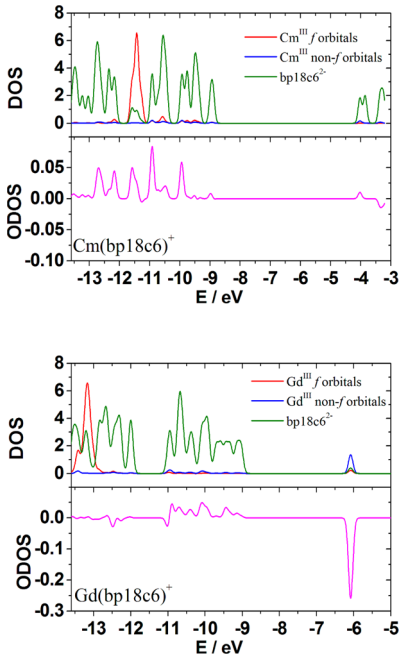

Figure 6. α-Spin density-of-states (DOS) and overlap population density-of-states (ODOS) of (*top panel*) $Cm(bp18c6)^+$ and (*bottom panel*) $Gd(bp18c6)^+$ complexes. A positive value in an ODOS plot represents bonding, whereas a negative value represents antibonding; a value that is close to zero indicates no bonding between molecular fragments.

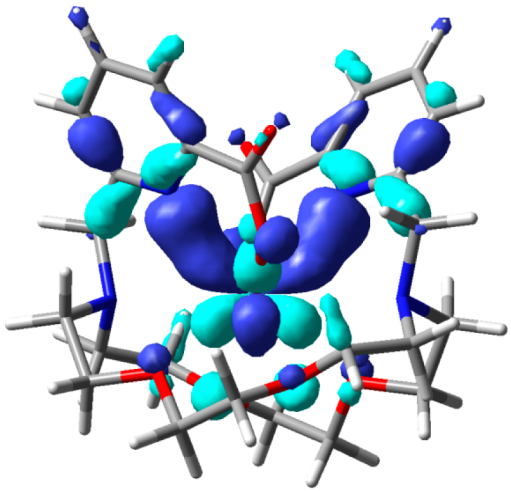

Figure 7. Surface plot of α-MO number 138 in $Cm(bp18c6)^+$.

138 (−11.59 eV), which is composed of a 67.9% contribution from metal 5f orbitals and a 31.1% ligand contribution and provides the strongest Cm–ligand covalent contribution involving occupied 5f orbitals, according to the ODOS analysis. As observed from Figure 7, MO 138 features an important overlap of the metal 5f orbital and the nitrogen atoms of the pyridyl groups. Additionally, the ODOS plot indicates an important contribution to covalent metal–ligand bonding of α MOs 132 (−12.59 eV), 145 (−10.92 eV), 146 (−10.91 eV), and 153 (−9.94 eV). The latter three MOs present non-negligible f contributions (3.9–5.4%) and comparable d metal contributions (2.5–5.9%).

Unlike the Cm^{III} complex, the ODOS and DOS plots shown in Figure 6 indicate that the 4f orbitals of Gd^{III} are not

dx.doi.org/10.1021/ic500244p | Inorg. Chem. 2014, 53, 6003–6012

significantly involved in covalent interactions with the ligand donor atoms. The most positive ODOS values for the Gd^{III} complex are obtained for MOs 146 (−10.91 eV) and 153 (−10.11 eV), which contain significant contributions from the non-f orbitals of gadolinium (7.3 and 5.4%, respectively) but negligible contributions from the 4f orbitals (0.3%). Thus, if covalent bonding has a measurable impact on the structure of $Ln(bp18c6)^+$ complexes, it is likely due to overlap of ligand orbitals and the lanthanide 5d orbitals rather than participation of lanthanide 4f orbitals in chemical bonding.[46] However, the 5f orbitals appear to play an important role in the bonding of An^{III}–$bp18c6^{2-}$ complexes, which is in line with previous studies. For instance, it was shown that ligand orbitals do not contribute to the frontier MOs with important 4f metallic character in Nd^{III} tris(dithiolene), while in the U^{III} system these orbitals are delocalized over the metal and the ligands and contain a substantial 5f contribution.[47]

DISCUSSION

Our equilibrium distribution and spectrophotometric experiments yield similar pictures of the stoichiometry and strength of the $An(bp18c6)^+$ complexes. In contrast to simple (neutral) crown ethers,[48,49] $bp18c6^{2-}$ is a potent ligand for An^{III} cations in aqueous solution, forming Am complexes that are almost as stable as $Am(edta)^-$.[12] The $M(bp18c6)^+$ stability constants in 1 M $NaNO_3$ (Table 1) also are greater than expected based on those previously reported for $Ln(bp18c6)^+$ complexation in 0.1 M KCl ($\log \beta_{101}$ for Eu^{III} = 14.29 in 1 M $NaNO_3$ vs 13.01 in 0.1 M KCl).[15] For Am and Cm, the electronic structure calculations suggest that a portion of the increased stability should arise from more covalent An^{III}–ligand interactions. However, the larger β_{101} value measured for $Eu(bp18c6)^+$ in 1 M $NaNO_3$ as compared to 0.1 M KCl indicates that medium-specific effects also contribute to the difference. A major source of this increased affinity of $bp18c6^{2-}$ for Eu^{III} appears to be the enhanced basicity of the ligand[50] in 1 M $NaNO_3$ relative to media with 0.1 M K^+ electrolyte solutions (Table 1), which is consistent with the significantly greater affinity of 18-crown-6 moieties for K^+ than for Na^+ in aqueous solution.[49,51]

In moderately acidic solutions (pcH ∼ 3) where an Am/Cm separation with $bp18c6^{2-}$ would be conducted, both $An(bp18c6)^+$ and $An(Hbp18c6)^{2+}$ are important species (Figure S3, Supporting Information). The protonation constants of the $An(bp18c6)^+$ complexes ($\log \beta_{111} - \log \beta_{101}$) derived from our data are 2.2 ± 0.2 for $Am(bp18c6)^+$ and 2.78 ± 0.09 for $Cm(bp18c6)^+$. They are similar to the protonation constants reported from potentiometric titrations of $Nd(bp18c6)^+$ and $Sm(bp18c6)^+$ in 0.1 M KCl, which are 2.08 and 2.70, respectively.[15] These low pK_a values underscore the difficulty of protonating the $M(bp18c6)^+$ complexes.

As a ligand, $bp18c6^{2-}$ shows unprecedented size-based selectivity for Am^{III} over Cm^{III} in a binary metal–ligand complex. The selectivity of $bp18c6^{2-}$ for Am is conveniently defined by the ratio of the Am and Cm stability constants (β_{101} Am/β_{101} Cm), which is 4.1 (3.5 kJ·mol^{-1}). This is similar to the selectivity of $bp18c6^{2-}$ previously reported for the similarly sized lanthanides Nd^{III} and Sm^{III}, 3.6,[15] and it represents a 5 kJ·mol^{-1} reversal in the expected selectivity patterns in which ligands favor Cm^{III} over Am^{III}. The Am/Eu selectivity of $bp18c6^{2-}$ is larger still (β_{101} Am/β_{101} Eu = 19), showing both the desired size-based selectivity and selectivity between An^{III} and Ln^{III} ions arising from enhanced interactions between the actinides and the nitrogen donor atoms of the ligand.[41,52]

The An^{III}/Ln^{III} selectivity of $bp18c6^{2-}$ is illustrated in Figure 8 where the distribution ratios of Am, Cm, and the light

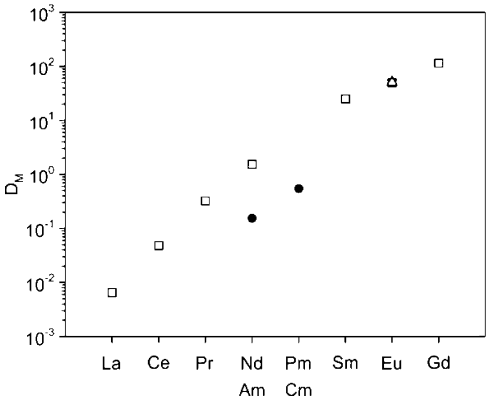

Figure 8. Separation of An^{III} and Ln^{III} by the system 0.05 M Hdehp in o-xylene/0.001 M $H_2bp18c6$ in 1 M $NaNO_3$, 0.05 M lactate at pcH 3.00 and 23 °C: (□) lanthanides measured by ICP-MS, (△) radiotracer Eu, (●) radiotracer actinides.

lanthanides are compared. If the selectivity of the aqueous ligand for An^{III} and Ln^{III} is solely a function of cation size, similarly sized An^{III} and Ln^{III} (i.e Am and Nd) would not be separated by this extraction system. Instead, the data in Figure 8 imply that the $Am(bp18c6)^+$ stability constants are an order of magnitude larger than the $Nd(bp18c6)^+$ stability constants (i.e., D_{Nd}/D_{Am} = 10) even though the metal cations are the same size. The DFT computations support this conclusion, indicating that the preference of $bp18c6^{2-}$ for actinide cations over similarly sized lanthanide cations appears to be due to interactions of the An^{III} with ligand nitrogen donor atoms, most notably the pyridine nitrogens.

Although the inherent Am^{III}/Cm^{III} selectivity of $bp18c6^{2-}$ falls short of our goal of 6–12 kJ·mol^{-1} (i.e., selectivity of 10–100 at 25 °C), the distribution experiments illustrate a realistic approach to improving the overall Am selectivity in a liquid–liquid extraction system. The aqueous solubilities of the ligand and its metal complexes function to preferentially retain Am in the aqueous phase. Therefore, pairing $bp18c6^{2-}$ with an organophillic ligand that preferentially extracts Cm^{III} over Am^{III}, such as Hdehp,[53] should increase the separation between Am and Cm by decreasing the relative concentration of Cm in the aqueous phase. This was actually the case in the extraction experiments where the overall separation factor between Cm and Am (D_{Cm}/D_{Am}) reached 6.5 (4.6 kJ·mol^{-1}) due to the additional, intrinsic selectivity of Hdehp for trivalent curium. With this additional selectivity, an aqueous solution containing 99% Am and 1% Cm could be produced from a 50:50 aqueous mixture of Am^{III} and Cm^{III} in as few as six repeated extraction stages using Hdehp as the extractant in the organic phase and $H_2bp18c6$ in the aqueous phase.

Given the potential of $bp18c6^{2-}$ for separating Am from Cm, we sought to understand whether the ligand's preference for Am^{III} over Cm^{III} was driven by the same structural features that cause its preference for larger Ln^{III} cations. Could the putative enhanced actinide–nitrogen interactions in the $An(bp18c6)^+$ complexes indirectly impact the mechanisms of size selectivity by distorting the structures of the actinide complexes relative to their lanthanide counterparts? Comparison of the apparent radii of the different ligand donor atoms across the series of $M(bp18c6)^+$ complexes we studied by DFT offers a way of

dx.doi.org/10.1021/ic500244p | Inorg. Chem. 2014, 53, 6003–6012

assessing these subtle effects. The apparent donor atom radius is the difference between the metal−ligand distance of a particular donor atom and the crystallographic radius of the metal. The apparent radius should be constant for similar metal complexes when the donor groups are free to adopt the most favorable metal−ligand binding geometry possible. The computations suggest there is no substantial difference in the behavior of the An^{III} and Ln^{III} because there is no systematic difference in the apparent donor radii of the $An(bp18c6)^{+}$ and $Ln(bp18c6)^{+}$ complexes (Figure 9).

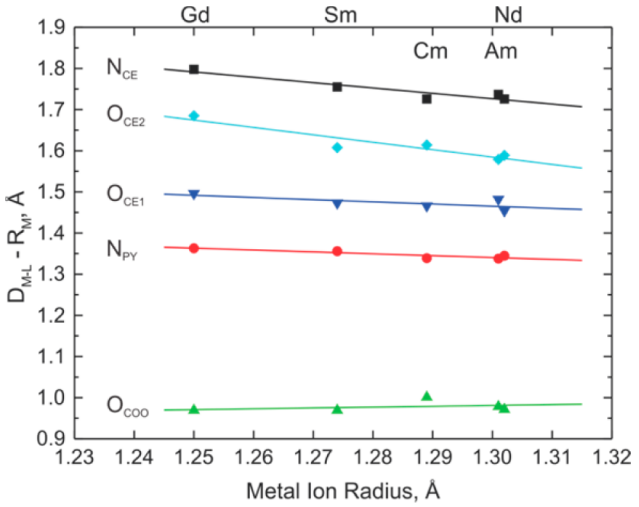

Figure 9. Apparent donor radii ($D_{M-L} - R_M$) of the crown ether donor atoms N_{CE} and O_{CE2} increase as the radius of the metal ion (R_M) decreases, indicating weaker interactions with smaller metal ions, while the apparent radii of donor atoms in the pyridine arms, N_{PY} and O_{COO}, change little. See Figure 5 for the identity of each donor atom.

The apparent radii also indicate that the Am/Cm size selectivity of $bp18c6^{2-}$ arises from the same steric constraints that drive its selectivity for larger Ln^{III} ions. The apparent radii of three sets of ligand donor atoms (O_{COO}, N_{PY}, and O_{CE1}) change little (0.01−0.04 Å) when the metal radii are systematically varied (Figure 9), implying that these donor atoms are comparatively free to adapt to the variations in f-element cation size. However, the apparent radii of two sets of ligand atoms in the crown ether ring (N_{CE}, O_{CE2}) increase with decreasing metal size, increasing by 0.06 and 0.1 Å as the cation radius decreases by 0.05 Å. These trends in the calculated apparent donor radii are supported by the crystal structures of the Gd^{III} and Yb^{III} complexes of $bp18c6^{2-}$.[15] They are also consistent with the presence of strong steric constraints that inhibit these donors from achieving the most favorable interaction geometries with smaller An^{III} and Ln^{III} cations and favor complexation of the larger Am^{III} cation over Cm^{III} and Ln^{III} cations smaller than Am^{III}. Thus, interactions between the metal ions and N_{CE} and O_{CE2} appear central to the ability of $bp18c6^{2-}$ to discriminate between similarly sized f-element cations, while interactions with N_{PY} impart group selectivity between An^{III} and Ln^{III}.

CONCLUSIONS

Combining relatively rigid 6-carboxy-2-pyridylmethyl groups with the inherently constrained diaza-18-crown-6 moiety produces a ligand that favors complexation of Am^{III} over Cm^{III} based on cation size, reversing the usual selectivity order for trivalent actinide cations. The measured Am/Cm selectivity of $bp18c6^{2-}$, 4.1, is the largest reported for binary An^{III}−ligand complexes. The overall stability of the $bp18c6^{2-}$ complexes and the Am/Cm selectivity are sufficient to allow reasonable separations of Am from Cm by conventional liquid−liquid extraction in mildly acidic solutions without having to oxidize Am or resort to chromatographic separations.

Furthermore, these metal binding constants and electronic structure calculations imply that the pyridine nitrogen donor atoms of the $bp18c6^{2-}$ ligand form more covalent bonds with An^{III} cations than with the equivalent Ln^{III} cations, resulting in thermodynamically stronger $An(bp18c6)^{+}$ complexes. This suggests that simultaneous separation of Am^{III} from Cm^{III} and lanthanide fission products may be possible with $bp18c6^{2-}$ or similar ligands. We are pursuing $H_2bp18c6$ derivatives with still greater Am^{III}/Ln^{III} selectivity based on these insights into the steric and electronic origins of f-element−$bp18c6^{2-}$ binding.

ASSOCIATED CONTENT

Supporting Information

Additional experimental details, extraction data, spectrophotometric fitting results, speciation diagrams, assessment of spin contamination, and listings of Cartesian coordinates of the $M(bp18c6)^{+}$ complexes *in vacuo*. This material is available free of charge via the Internet at http://pubs.acs.org.

AUTHOR INFORMATION

Corresponding Authors

*E-mail: mjensen@anl.gov.
*E-mail: mayter@udc.es.

Notes

The authors declare no competing financial interest.

ACKNOWLEDGMENTS

Work at Argonne (contract number DE-AC02-06CH11357) and UWM was supported by the U.S. Department of Energy, Assistant Secretary of the Office of Nuclear Energy, Fuel Cycle Research and Development Program. A.R.-S., A.d.B., C.P.-I., and T.R.-B. thank Xunta de Galicia (CN 2012/011) for generous financial support and Centro de Supercomputación de Galicia (CESGA) for providing the computer facilities.

REFERENCES

(1) (a) Pillon, S.; Somers, J.; Grandjean, S.; Lacquement, J. *J. Nucl. Mater.* **2003**, *320*, 36−43. (b) Lebreton, F.; Prieur, D.; Horlait, D.; Delahaye, T.; Jankowiak, A.; Léorier, C.; Jorion, F.; Gavilan, E.; Desmoulière, F. *J. Nucl. Mater.* **2013**, *438*, 99−107. (c) Bays, S.; Piet, S.; Pope, M.; Youinou, G.; Dumontier, A.; Hawn, D. *Transmutation Dynamics: Impacts of Multi-Recycling on Fuel Cycle Performances*; Idaho National Laboratory: Idaho Falls, ID, 2009. (d) Salvatores, M.; Palmiotti, G. *Prog. Part. Nucl. Phys.* **2011**, *66*, 144−166.

(2) Nash, K. L.; Madic, C.; Mathur, J. N.; Lacquement, J., Actinide Separation Science and Technology. In *The Chemistry of the Actinide and Transactinide Elements*; Morss, L. R., Edelstein, N. M., Fuger, J., Eds.; Springer: Dordrecht, The Netherlands, 2006; Vol. *4*, pp 2622−2798.

(3) Runde, W. H.; Mincher, B. J. *Chem. Rev.* **2011**, *111*, 5723−5741.

(4) Burns, J. D.; Shehee, T. C.; Clearfield, A.; Hobbs, D. T. *Anal. Chem.* **2012**, *84*, 6930−6932.

(5) (a) Kraak, W.; Van Der Heijden, W. A. *J. Inorg. Nucl. Chem.* **1966**, *28*, 221−224. (b) Felker, L. K.; Benker, D. E.; Chattin, F. R.; Stacy, R. G. *Sep. Sci. Technol.* **1995**, *30*, 1769−1778. (c) Suzuki, T.; Fujii, Y.; Koyama, S.-i.; Ozawa, M. *Prog. Nucl. Energy* **2008**, *50*, 456−461.

(d) Koyama, S.; Ozawa, M.; Suzuki, T.; Fujii, Y. *J. Nucl. Sci. Technol.* **2006**, *43*, 681−689.
(6) Mincher, B. J.; Martin, L. R.; Schmitt, N. C. *Inorg. Chem.* **2008**, *47*, 6984−6989.
(7) Modolo, G.; Kluxen, P.; Geist, A. *Radiochim. Acta* **2010**, *98*, 193−201.
(8) David, F. *J. Less-Common Met.* **1986**, *121*, 27−42.
(9) (a) Kirker, I.; Kaltsoyannis, N. *Dalton Trans.* **2011**, *40*, 124−131. (b) Ingram, K. I. M.; Tassell, M. J.; Gaunt, A. J.; Kaltsoyannis, N. *Inorg. Chem.* **2008**, *47*, 7824−7833. (c) Guillaumont, D. *THEOCHEM* **2006**, *771*, 105−110.
(10) (a) Choppin, G. R.; Jensen, M. P. Actinides in Solution: Complexation and Kinetics. In *The Chemistry of the Actinide and Transactinide Elements*; Morss, L. R., Edelstein, N. M.; Fuger, J., Eds.; Springer: Dordrecht, The Netherlands, 2006; Vol. *4*, pp 2524−2621. (b) Nash, K. L.; Jensen, M. P. *Sep. Sci. Technol.* **2001**, *36*, 1257−1282.
(11) (a) Küchle, W.; Dolg, M.; Stoll, H. *J. Phys. Chem. A* **1997**, *101*, 7128−7133. (b) Laerdahl, J. K.; Fægri, K.; Visscher, L.; Saue, T. *J. Chem. Phys.* **1998**, *109*, 10806−10817.
(12) Smith, R. M.; Martell, A. E.; Motekaitis, R. J. *Critically Selected Stability Constants of Metal Complexes Database Version 8.0*; NIST Standard Reference Data: Gaithersburg, MD, 2004; Vol. *46*.
(13) (a) Ahrland, S. Solution Chemistry and Kinetics of Ionic Reactions. In *Chemistry of the Actinide Elements*; Katz, J. J., Seaborg, G. T., Morss, L. R., Eds.; Chapman and Hall: New York, 1986; Vol. *2*, p 1497. (b) Myasoedov, B. F.; Guseva, L. I.; Lebedev, I. A.; Milyukova, M. S.; Chmutova, M. K. *Analytical Chemistry of Transplutonium Elements*; Halsted Press: New York, 1974; pp 234−318.
(14) Leggett, C. J.; Jensen, M. P. *J. Solution Chem.* **2013**, *42*, 2119−2136.
(15) Roca-Sabio, A.; Mato-Iglesias, M.; Esteban-Gomez, D.; Toth, E.; de Blas, A.; Platas-Iglesias, C.; Rodriguez-Blas, T. *J. Am. Chem. Soc.* **2009**, *131*, 3331−3341.
(16) (a) Tei, L.; Baranyai, Z.; Brücher, E.; Cassino, C.; Demicheli, F.; Masciocchi, N.; Giovenzana, G. B.; Botta, M. *Inorg. Chem.* **2010**, *49*, 616−625. (b) Roca-Sabio, A.; Mato-Iglesias, M.; Esteban-Gomez, D.; De Blas, A.; Rodriguez-Blas, T.; Platas-Iglesias, C. *Dalton Trans.* **2011**, *40*, 384−392.
(17) Nash, K. L. *Solvent Extr. Ion Exch.* **1993**, *11*, 729−768.
(18) Partridge, J. A.; Jensen, R. C. *J. Inorg. Nucl. Chem.* **1969**, *31*, 2587−2589.
(19) Chiarizia, R.; Jensen, M. P.; Borkowski, M.; Ferraro, J. R.; Thiyagarajan, P.; Littrell, K. C. *Sep. Sci. Technol.* **2003**, *38*, 3313−3331.
(20) Özçubukçu, S.; Mandal, K.; Wegner, S.; Jensen, M. P.; He, C. *Inorg. Chem.* **2011**, *50*, 7937−7939.
(21) Jensen, M. P.; Nash, K. L. *Radiochim. Acta* **2001**, *89*, 557−564.
(22) (a) Becke, A. D. J. *J. Chem. Phys.* **1993**, *98*, 5648−5652. (b) Lee, C.; Yang, W.; Parr, R. G. *Phys. Rev. B* **1988**, 785−789.
(23) Frisch, M. J.; Trucks, G. W.; Schlegel, H. B.; Scuseria, G. E.; Robb, M. A.; Cheeseman, J. R.; Scalmani, G.; Barone, V.; Mennucci, B.; Petersson, G. A.; Nakatsuji, H.; Caricato, M.; Li, X.; Hratchian, H. P.; Izmaylov, A. F.; Bloino, J.; Zheng, G.; Sonnenberg, J. L.; Hada, M.; Ehara, M.; Toyota, K.; Fukuda, R.; Hasegawa, J.; Ishida, M.; Nakajima, T.; Honda, Y.; Kitao, O.; Nakai, H.; Vreven, T.; Montgomery, J. A., Jr.; Peralta, J. E.; Ogliaro, F.; Bearpark, M.; Heyd, J. J.; Brothers, E.; Kudin, K. N.; Staroverov, V. N.; Kobayashi, R.; Normand, J.; Raghavachari, K.; Rendell, A.; Burant, J. C.; Iyengar, S. S.; Tomasi, J.; Cossi, M.; Rega, N.; Millam, N. J.; Klene, M.; Knox, J. E.; Cross, J. B.; Bakken, V.; Adamo, C.; Jaramillo, J.; Gomperts, R.; Stratmann, R. E.; Yazyev, O.; Austin, A. J.; Cammi, R.; Pomelli, C.; Ochterski, J. W.; Martin, R. L.; Morokuma, K.; Zakrzewski, V. G.; Voth, G. A.; Salvador, P.; Dannenberg, J. J.; Dapprich, S.; Daniels, A. D.; Farkas, Ö.; Foresman, J. B.; Ortiz, J. V.; Cioslowski, J.; Fox, D. J. *Gaussian 09*, Revision A.02; Gaussian, Inc.: Wallingford, CT, 2009.
(24) (a) Kuechle, W.; Dolg, M.; Stoll, H.; Preuss, H. *J. Chem. Phys.* **1994**, *100*, 7535−7542. (b) Cao, X.; Dolg, M.; Stoll, H. *J. Chem. Phys.* **2003**, *118*, 487−496. (c) Cao, X.; Dolg, M. *J. Mol. Struct. (THEOCHEM)* **2004**, *673*, 203−209.
(25) Cao, X.; Dolg, M. *J. Mol. Struct. (THEOCHEM)* **2002**, *581*, 139−147.
(26) Dolg, M.; Stoll, H.; Preuss, H. *J. Chem. Phys.* **1989**, *90*, 1730−1734.
(27) Stanton, J. F.; Gauss, J. *Adv. Chem. Phys.* **2003**, *125*, 101−146.
(28) Montoya, A.; Truong, T. N.; Sarofim, A. F. *J. Phys. Chem. A* **2000**, *124*, 6108−6110.
(29) Zekany, L.; Nagypal, I. PSEQUAD: A Comprehensive Program for the Evaluation of Potentiometric and/or Spectrophotometric Equilibrium Data Using Analytical Derivatives. In *Computational Methods for the Determination of Formation Constants*, Leggett, D. J., Ed.; Plenum Press: New York, 1985.
(30) Ferreirós-Martínez, R.; Esteban-Gómez, D.; Tóth, E.; de Blas, A.; Platas-Iglesias, C.; Rodríguez-Blas, T. *Inorg. Chem.* **2011**, *50*, 3772−3784.
(31) Jensen, M. P.; Rickert, P. G.; Schmidt, M. A.; Nash, K. L. *J. Alloys Compd.* **1997**, *249*, 86−90.
(32) Aguilar, M. Graphical treatment of liquid-liquid equilibrium data. In *Developments in Solvent Extraction*; Alegret, S., Ed.; Ellis Horwood: West Sussex, England, 1988; pp 87−118.
(33) Nash, K. L. *Radiochim. Acta* **1991**, *54*, 171−179.
(34) Shanbhag, S. M.; Choppin, G. R. *Inorg. Chem.* **1982**, *21*, 1696−1697.
(35) Malinowski, E. R. *Factor Analysis in Chemistry*; Wiley: New York, 2002.
(36) Hartley, F. R.; Burgess, C.; Alcock, R. M. *Solution Equilibria*; Ellis Horwood Ltd.: Chichester, England, 1980.
(37) Leggett, D. J. SQUAD: Stability Quotients from Absorbance Data. In *Computational Methods for the Determination of Formation Constants*; Leggett, D. J., Ed.; Plenum Press: New York, 1985; pp 159−220.
(38) Ferreirós-Martínez, R.; Esteban-Gómez, D.; de Blas, A.; Platas-Iglesias, C.; Rodríguez-Blas, T. *Inorg. Chem.* **2009**, *48*, 11821−11831.
(39) Dolg, M.; Stoll, H.; Savin, A.; Preuss, H. *Theor. Chim. Acta* **1989**, *75*, 173−194.
(40) (a) Kaltsoyannis, N. *Inorg. Chem.* **2013**, *52*, 3407−3413. (b) Neidig, M. L.; Clark, D. L.; Martin, R. L. *Coord. Chem. Rev.* **2013**, *257*, 394−406. (c) Minasian, S. G.; Krinsky, J. L.; Rinehart, J. D.; Copping, R.; Tyliszczak, T.; Janousch, M.; Shuh, D. K.; Arnold, J. *J. Am. Chem. Soc.* **2009**, *131*, 13767−13783. (d) Arliguie, T.; Belkhiri, L.; Bouaoud, S.-E.; Thuéry, P.; Villiers, C.; Boucekkine, A.; Ephritikhine, M. *Inorg. Chem.* **2008**, *48*, 221−230. (e) Roger, M.; Barros, N.; Arliguie, T.; Thuéry, P.; Maron, L.; Ephritikhine, M. *J. Am. Chem. Soc.* **2006**, *128*, 8790−8802. (f) Petit, L.; Borel, A.; Daul, C.; Maldivi, P.; Adamo, C. *Inorg. Chem.* **2006**, *45*, 7382−7388. (g) Gaunt, A. J.; Reilly, S. D.; Enriquez, A. E.; Scott, B. L.; Ibers, J. A.; Sekar, P.; Ingram, K. I. M.; Kaltsoyannis, N.; Neu, M. P. *Inorg. Chem.* **2007**, *47*, 29−41. (h) Vetere, V.; Maldivi, P.; Adamo, C. *J. Comput. Chem.* **2003**, *24*, 850−858. (i) Ingram, K. I. M.; Tassell, M. J.; Gaunt, A. J.; Kaltsoyannis, N. *Inorg. Chem.* **2008**, *47*, 7824−7833.
(41) Miguirditchian, M.; Guillaneux, D.; Guillaumont, D.; Moisy, P.; Madic, C.; Jensen, M. P.; Nash, K. L. *Inorg. Chem.* **2005**, *44*, 1404−1412.
(42) Shannon, R. D. *Acta Crystallogr.* **1976**, *A32*, 751−767.
(43) (a) Corey, E. J.; Bailar, C. J., Jr. *J. Am. Chem. Soc.* **1959**, *81*, 2620−2629. (b) Beattie, J. K. *Acc. Chem. Res.* **1971**, *4*, 253−259.
(44) Cioslowski, J. *J. Am. Chem. Soc.* **1989**, *111*, 8333−8336.
(45) (a) Grorelsky, S. I.; Ghosh, S.; Solomon, E. I. *J. Am. Chem. Soc.* **2006**, *128*, 278−290. (b) Platas-Iglesias, C.; Esteban-Gomez, D.; Enríquez-Pérez, T.; Avecilla, F.; de Blas, A.; Rodriguez-Blas, T. *Inorg. Chem.* **2005**, *44*, 2224−2233.
(46) Krough-Jespersen, K.; Romanelli, M. D.; Melman, J. H.; Emge, T. J.; Brennan, J. G. *Inorg. Chem.* **2010**, *49*, 552−560.
(47) Meskaldji, S.; Belkhiri, L.; Arliguie, T.; Fourmigué, M.; Ephritikhine, M. *Inorg. Chem.* **2010**, *49*, 3192−3200.
(48) (a) Izatt, R. M.; Pawlak, K.; Bradshaw, J. S.; Bruening, R. L. *Chem. Rev.* **1995**, *95*, 2529−2586. (b) Izatt, R. M.; Pawlak, K.; Bradshaw, J. S.; Bruening, R. L. *Chem. Rev.* **1991**, *91*, 1721−2085. (c) Tsurubou, S.; Mizutani, M.; Kadota, Y.; Yamamoto, T.; Umetani,

S.; Sasaki, T.; Le, Q. T. H.; Matsui, M. *Anal. Chem.* **1995**, *67*, 1465−1469. (d) Sasaki, T.; Umetani, S.; Matsui, M.; Tsurubou, S.; Kinura, T.; Yoshida, Z. *Bull. Chem. Soc. Jpn.* **1998**, *71*, 371−377.
(49) Izatt, R. M.; Bradshaw, J. S.; Nielsen, S. A.; Lamb, J. D.; Christensen, J. J.; Sen, D. *Chem. Rev.* **1985**, *85*, 271−339.
(50) Choppin, G. R. *J. Alloys Compd.* **1995**, *223*, 174−179.
(51) Buschmann, H. J.; Cleve, E.; Schollmeyer, E. *J. Coord. Chem.* **1996**, *39*, 293−298.
(52) (a) Musikas, C. Actinide-Lanthanide Group Separation using Sulfur and Nitrogen Donor Extractants. In *International Symposium on Actinide/Lanthanide Separations*; Choppin, G. R., Navratil, J. D., Schulz, W. W., Eds.; World Scientific: Philadelphia, 1984; pp 19−30. (b) Jensen, M. P.; Morss, L. R.; Beitz, J. V.; Ensor, D. D. *J. Alloys Compd.* **2000**, *303/304*, 137−141.
(53) Mason, G. W.; Metta, D. N.; Peppard, D. F. *J. Inorg. Nucl. Chem.* **1976**, *38*, 2077−2079.